

Crystal-structure refinements for orthorhombic boracite, $\text{Mg}_3\text{ClB}_7\text{O}_{13}$, and a trigonal, iron-rich analogue*

By ERIC DOWTY** and JOAN R. CLARK

U. S. Geological Survey, Washington, D.C.

(Received 13 October 1972)

Auszug

Die Kristallstrukturen des rhombischen Boracits, $\text{Mg}_3\text{B}_7\text{O}_{13}\text{Cl}$, und seines eisenreichen trigonalen Analogons $\text{Fe}_{2,4}\text{Mg}_{0,6}\text{B}_7\text{O}_{13}\text{Cl}$ wurden auf Grund von 1509 Interferenzen für den ersten ($Pca\ 2_1$, $a = b = c/\sqrt{2} = 8,5496 \text{ \AA}$, $c = 12,0910 \pm 0,0009 \text{ \AA}$, $Z = 4$) und 650 Interferenzen für das zweite ($R3c$, $a = 8,612 \pm 0,002 \text{ \AA}$, $c = 21,065 \pm 0,004 \text{ \AA}$, $Z = 6$) bis zu $R = 0,038$ bzw. $0,065$ verfeinert. Die zwei Strukturen sind sehr ähnlich; sie unterscheiden sich nur in der Anordnung der symmetrisch-äquivalenten Einheiten. Sie haben ein zusammenhängendes B-O-Gerüst mit großen Zwischenräumen, in denen sich die Kationen und das Cl-Atom befinden. Das Gerüstmuster besteht aus drei Ringen, die drei B-O-Tetraedern angehören, welche sich in einem gemeinsamen O-Atom, O(1) berühren. Die Ringsysteme sind direkt oder über ein einzelnes B-O-Dreieck miteinander räumlich verknüpft. Das Atom O(1) ist nicht, wie früher beschrieben, vier „ BO_3O -Pyramiden“ gemeinsam, sondern drei dieser „Pyramiden“ sind normale Tetraeder und das vierte ein Dreieck. Die Mg- und Fe-Atome sind fünf-fach-koordiniert; das sie umgebende Polyeder läßt sich am besten als ein Übergang zwischen tetragonaler Pyramide und trigonaler Bipyramide beschreiben. Die ungewöhnliche Koordination und einige anomale Kation-Chlor-Abstände sind wahrscheinlich durch die Art der Hohlräume bedingt. Bei den meisten Verbindungen mit boracitähnlicher Struktur und mit verschiedenen Kationen und Halogenen als Ersatz für Mg und Cl wurde ein Ansteigen der ferroelektrischen Umwandlungstemperatur mit wachsendem Verhältnis des Ionenradius von Me^{+2} gegenüber dem des Halogens gefunden.

Abstract

The crystal structures of orthorhombic boracite, $\text{Mg}_3\text{ClB}_7\text{O}_{13}$, and of a trigonal iron-rich analogue, $\text{Fe}_{2,4}\text{Mg}_{0,6}\text{ClB}_7\text{O}_{13}$, have been refined using 1509

* *Dedicated to Professor M. J. Buerger on the occasion of his 70th birthday.* Publication authorized by the Director, U. S. Geological Survey, Washington, D.C. 20242.

** Present address: Department of Geology and Institute of Meteoritics, University of New Mexico, Albuquerque, New Mexico 87106.

reflections for boracite ($Pca2_1$, $a = b = c/\sqrt{2} = 8.5496 \text{ \AA}$, $c = 12.0910 \pm 0.0009 \text{ \AA}$, $Z = 4$) and 650 reflections for the analogue ($R3c$, $a = 8.612 \pm 0.002 \text{ \AA}$, $c = 21.065 \pm 0.004 \text{ \AA}$, $Z = 6$). The residuals R are, respectively, 0.038 and 0.065. The two structures are quite similar, differing only in the arrangement of symmetry-equivalent units. They consist of unbroken boron-oxygen frameworks with large interstices in which the metal cations and chloride anions reside. The basic unit of the borate framework is made up of three rings of three boron-oxygen tetrahedra sharing corners and joined at a common oxygen atom, O(1); the ring systems are cross-linked to one another, as well as through a single boron-oxygen triangle. The O(1) oxygen atom is not common to four "BO₃O pyramids", as previously described. Instead one of these four is a normal triangle and the other three are normal tetrahedra. Magnesium and iron cations are five coordinated in an arrangement best described as transitional between square pyramidal and trigonal bipyramidal. The nature of the cavities in the borate framework probably accounts for the unusual coordination and some anomalous cation-chlorine distances. For most compounds with boracite-like structures, in which various cations substitute for magnesium and various halogens for chlorine, the ferroelectric transition temperature is found to increase with the ionic radius ratio, $Me^{2+}/\text{halogen}$.

Introduction

The interesting "ferro" effects in boracite structures have recently been discussed by a number of authors; for example, the ferroelectric properties by SCHMID (1965, 1970), SCHMID and TROOSTER (1967), KOBAYASHI *et al.* (1968), and ZIMMERMAN *et al.* (1970), to name just a few; the ferromagnetic properties by ASCHER *et al.* (1966); and the ferroelastic properties by AIZU (1968) and TORRE *et al.* (1972). In addition, some optical properties have been discussed by DORMANN (1970), and thermodynamic properties by DVORAK (1971). We cannot hope to mention here all the vast literature which has come out on the boracite-like structures in the past few years.

The structures of boracite and its many synthetic analogues have been assumed to be essentially as described in 1951 by ITO, MORIMOTO, and SADANAGA for the cubic and orthorhombic forms of boracite, Mg₃ClB₇O₁₃. The observed ferroelectric effects have been attributed entirely to movements of metal and halogen atoms, and the borate framework has been assumed "not responsible for the ferroelectricity" (ZIMMERMAN *et al.*, 1970). However, certain features of the accepted structure appeared to be anomalous. The cubic structure, and the orthorhombic one as well, were originally described by ITO *et al.* (1951) as having "BO₃O pyramids", four such pyramids being linked through a common oxygen atom. Such coordination has not been encountered in any of the numerous borate structures studied since 1951, nor is it

compatible with the nuclear magnetic resonance spectra (BRAY *et al.*, 1961; KRIZ and BRAY, 1971). We therefore decided to re-examine the orthorhombic structure. Our results confirm the general features of the orthorhombic structure proposed by ITO *et al.* (1951) but important revisions of the boron-oxygen relationships reveal that there are no "pyramids" in the structure. We have also refined the structure of the trigonal iron-rich analogue¹, $\text{Fe}_{2.4}\text{Mg}_{0.6}\text{ClB}_7\text{O}_{13}$, and have found that the borate framework is essentially the same. A preliminary report on the borate framework has appeared (DOWTY and CLARK, 1972a), and a note concerned with the ferroelectric and ferroelastic aspects has been published (DOWTY and CLARK, 1972b). Prof. J. J. PAPIKE and Dr. SHIGEHO SUENO, State University of New York at Stony Brook, are collecting data above the orthorhombic-cubic transition temperature on the same boracite crystal used during this study, and their results will be published elsewhere.

Experimental work

Crystallographic and chemical data

The large (some greater than 0.5 cm diameter) crystals showing cubic morphology, in which boracite and its iron analogue are often found, are intensely twinned on a microscopic scale. To obtain material suitable for diffraction studies, it was necessary to crush these large pseudomorphs and select small untwinned fragments. The crystal of boracite selected for study was an irregular fragment with trapezoidal shape from a specimen originating at Solvayshall, Roschwitz, Germany (U. S. National Museum No. B 12325); the size of the fragment was $0.23 \times 0.16 \times 0.10$ mm. It was verified optically to be a single domain. The optical orientation is given in Table 1, together with the cell constants obtained from measurements of standard powder diffractometer data refined by least-squares methods (APPLEMAN *et al.*, in press). No chemical analysis was made during this study; the boracite is assumed to be almost pure.

The crystal of the iron-rich analogue originated at Bischofferode, Thüringen, Germany, and it was also an irregular fragment, 0.13×0.10

¹ The crystal was chosen from a sample labelled "ericaité" (HEIDE, 1955; KÜHN and SCHAACKE, 1955) and was thus designated in early notes (DOWTY and CLARK, 1972a,b). However, the nomenclature is uncertain following the recent description of "congolite" (WENDLING *et al.*, 1972). We therefore refer here to the "trigonal iron-rich analogue of boracite" rather than using either mineral name.

Table 1. *Crystallographic data for boracite and the iron-rich analogue*

Symmetry Space group	Boracite Orthorhombic <i>Pca 2₁</i>	Iron-rich analogue* Trigonal <i>R 3c</i>
Cell constants		
<i>a</i>	$c/\sqrt{2} = 8.5496$	$8.612 \pm 0.002 \text{ \AA}$
<i>b</i>	$c/\sqrt{2} = 8.5496$	$8.612 \pm 0.002 \text{ \AA}$
<i>c</i>	12.0910 ± 0.0009	$21.065 \pm 0.004 \text{ \AA}$
Cell volume	883.81	1353.0 \AA^3
<i>Z</i>	4 [Mg ₃ ClB ₇ O ₁₃]	6 [Fe _{2.4} Mg _{0.6} ClB ₇ O ₁₃]
Calc. density	2.945	3.443 g/cm ³
Optical orientation	$X = c, Y = a, Z = b$	

* Corrected from values given by DOWTY and CLARK (1972b).

$\times 0.07$ mm. Optical examination showed that this crystal contained from five to ten percent of a second domain with a different orientation. As no better crystal could be found, we assumed that the slight admixture would not cause major problems. Indeed the results do not seem to be those that would be expected for a superposition of structures due to undetected domains. Cell constants for this material, obtained as were those for boracite, are given in Table 1. From the previously published analysis (KÜHN and SCHAAKE, 1955), the crystal is assumed to have about twenty percent of the iron replaced by magnesium, so its formula is taken as Fe_{2.4}Mg_{0.6}ClB₇O₁₃. Careful examination of single-crystal precession photographs and monitoring of equivalent reflections during data collection revealed no departure from *R3c* symmetry.

Single-crystal x-ray diffraction data

Data for both crystals were collected on a Picker single-crystal automatic diffractometer by 2θ -scan methods, using Nb-filtered Mo x-radiation and a scintillation-counter detector. The scan range was calculated as suggested by ALEXANDER and SMITH (1964). Background counts of 20 seconds duration were made for each reflection at the beginning and end of the scan range. The boracite crystal was mounted with *b* parallel to the φ axis and 2621 reflections were measured. The iron-rich analogue was mounted with *c* parallel to the φ axis and 1591

reflections were measured. In each case a standard reflection was monitored after every 30 measurements.

Computer programs written by Prof. C. T. PREWITT, State University of New York at Stony Brook, and modified for the IBM 360/65 by D. E. APPLEMAN, U. S. Geological Survey, were used to obtain the diffractometer settings and to reduce the raw data, including corrections for the total background count and for Lorentz and polarization factors. No absorption corrections were made for boracite ($\mu = 7.6 \text{ cm}^{-1}$), or for the iron-rich analogue ($\mu = 43.6 \text{ cm}^{-1}$). The observed $|F_o|$ was less than four times its standard deviation from background as determined by the counting statistics for 1112 reflections of boracite and 841 reflections of the iron-rich analogue; these reflections were coded as "less-thans" and omitted during the refinements, which used 1509 reflections for boracite and 650 reflections for the trigonal analogue.

Refinement procedures

The computer program ORFLS (BUSING *et al.*, 1962) was used for preliminary refinement of boracite. Programs RFINE and BADTEA, written by Dr. L. W. FINGER, Geophysical Laboratory, Washington, D. C., were used for the final refinement of boracite and all refinement of the iron-rich form, as well as for calculation of bond distances, bond angles, and thermal ellipsoids. The scattering factors were calculated from a nine-coefficient analytical function (CROMER and WABER, 1965) using the coefficients given by CROMER and MANN (1968) for neutral atoms.

The atomic parameters given by ITO *et al.* (1951) were used initially for the orthorhombic boracite; four cycles of least-squares refinement for positional parameters and individual isotropic temperature factors reduced the conventional $R = \sum ||F_o| - |F_c|| / \sum |F_o|$ from 0.275 to 0.061, and nine more cycles refining anisotropic temperature parameters reduced R to 0.038. Six intense reflections presumed to be affected by extinction were removed after the sixth cycle. A three-dimensional electron-density Fourier synthesis and the associated difference Fourier synthesis were then calculated using the *X-Ray 67, Program system for x-ray crystallography* by J. M. STEWART, University of Maryland (adapted for the IBM 360/65 by D. E. APPLEMAN, U. S. Geological Survey). No unusual features were noted and the maximum difference observed was $\pm 0.7 \text{ e}/\text{\AA}^3$.

The locations of the (Fe,Mg) and Cl atoms in the iron-rich analogue were assumed to be as proposed by SCHMID (1970), but the locations

of the boron and oxygen atoms were derived by analogy with our previously refined structure of boracite. A total of nine cycles of refinement, the later ones with anisotropic temperature factors, reduced R to 0.065. The Fourier difference map showed features sometimes

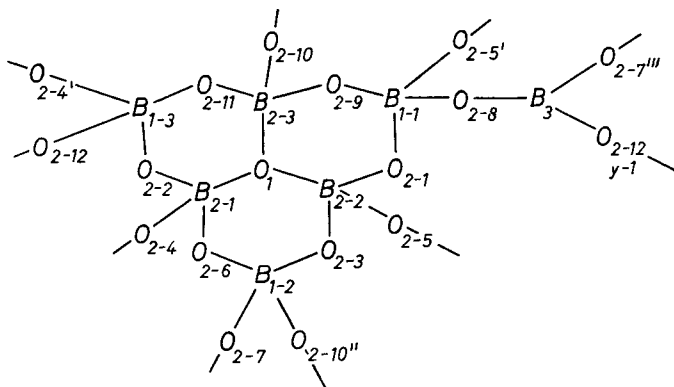


Fig. 1. Schematic diagram of the asymmetric unit that forms the borate framework in boracite and its analogue, numbered as for the orthorhombic structure (Table 2)

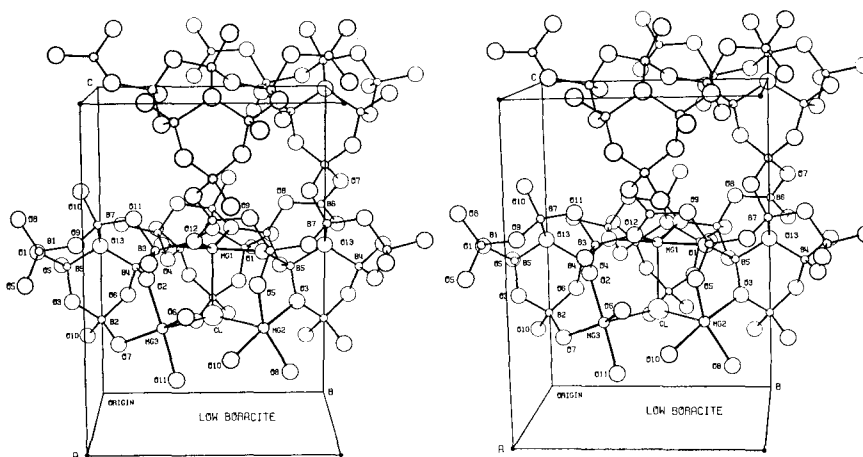


Fig. 2. Stereoscopic-pair view of selected portions of the borate framework in orthorhombic boracite. Atom labelling as follows: O(13) = O(1), others are O(2) atoms; B(1), B(2), B(3) are the B(1) set, B(4), B(5), B(7) are the B(2) set; B(6) = B(3). The close approach of B(3) to O(1) can be seen at mid-right between labelled B(6) and O(13). Drawing produced by ORTEP (JOHNSON, 1965)

Table 2. *Atomic and thermal parameters for orthorhombic*

Crystal	Atom	x	y	z	Equivalent isotropic B
O	Cl	0.0241 (1)	0.4994 (2)	0.2618	0.92 Å ²
T	Cl	0.0	0.0	0.2654 (2)	1.16
O	Mg(1)	-0.0083 (2)	0.4988 (3)	0.4770 (2)	0.59
T	(Fe,Mg)	0.1480 (4)	0.2971 (2)	0.3270	0.74
O	Mg(2)	0.2351 (2)	0.7204 (2)	0.2537 (2)	0.62
O	Mg(3)	0.2350 (2)	0.2784 (2)	0.2514 (2)	0.59
O	B(1)-1	0.2482 (7)	0.7483 (6)	0.5018 (5)	0.26
T	B(1)-1	0.162 (3)	-0.169 (3)	0.0828 (5)	0.59
O	B(1)-2	0.0060 (5)	0.9987 (9)	0.2488 (5)	0.43
O	B(1)-3	0.2481 (7)	1.2523 (7)	0.5016 (6)	0.46
O	B(2)-1	0.0023 (5)	1.1537 (7)	0.4202 (6)	0.46
T	B(2)	0.099 (2)	-0.105 (2)	-0.0286 (4)	0.78
O	B(2)-2	0.0035 (5)	0.8464 (7)	0.4224 (6)	0.50
O	B(2)-3	0.1553 (4)	0.9999 (6)	0.5735 (4)	0.50
O	B(3)	0.2972 (5)	0.5000 (7)	0.6012 (4)	0.51
T	B(3)	0.0	0.0	0.102 (1)	0.96
O	O(1)	0.0173 (3)	0.9993 (5)	0.4914 (3)	0.40
T	O(1)	0.0	0.0	-0.0126 (6)	0.70
O	O(2)-1	0.0824 (3)	0.7218 (4)	0.4794 (4)	0.34
T	O(2)-1	-0.160 (1)	-0.001 (1)	0.1056 (3)	0.59
O	O(2)-2	0.1606 (4)	1.2107 (4)	0.4019 (4)	0.39
T	O(2)-2	0.289 (1)	0.261 (1)	-0.0353 (3)	0.64
O	O(2)-3	0.0789 (3)	0.8753 (4)	0.3156 (4)	0.41
T	O(2)-3	0.199 (1)	-0.022 (1)	-0.0869 (3)	0.67
O	O(2)-4	-0.0857 (4)	1.2701 (4)	0.4813 (4)	0.41
T	O(2)-4	-0.306 (1)	-0.226 (1)	0.0204 (3)	0.66
O	O(2)-5	-0.1604 (4)	0.8072 (4)	0.4059 (4)	0.44
O	O(2)-6	-0.0730 (4)	1.1153 (4)	0.3172 (4)	0.50
O	O(2)-7	0.1330 (3)	1.0801 (4)	0.1865 (3)	0.38
O	O(2)-8	0.2885 (4)	0.6613 (3)	0.6066 (4)	0.52
O	O(2)-9	0.2837 (4)	0.9129 (4)	0.5226 (4)	0.29
O	O(2)-10	0.1109 (3)	0.9243 (4)	0.6764 (3)	0.33
O	O(2)-11	0.2004 (4)	1.1597 (3)	0.5965 (3)	0.35
O	O(2)-12	0.2075 (4)	0.4206 (4)	0.5261 (4)	0.45

greater than $\pm 1.0 e/\text{Å}^3$ at locations distinct from the final atomic positions. The locations of these features, however, could be rationalized on the basis of a "ghost" structure due to the presence of the second minor domain in a twin relationship.

The atomic parameters obtained are listed in Table 2 for both crystals, and the structure factors calculated with these parameters are

boracite (O) and an iron-rich, trigonal analogue (T)

Parameter* β_{11}	β_{22}	β_{33}	β_{12}	β_{13}	β_{23}
35 (1)	28 (1)	16 (1)	0.6 (1.4)	0.8 (7)	-0.6 (1.0)
50 (3)	50	7 (1)	25	0	0
15 (1)	13 (1)	16 (1)	-0.5 (1.0)	0.6 (1.3)	-2 (2)
34 (3)	38 (2)	3.8 (1)	19 (3)	1 (1)	3 (1)
23 (2)	21 (2)	10 (2)	9 (1)	0.3 (1.4)	-2 (1)
24 (2)	21 (2)	8 (2)	-9 (2)	2 (1)	-1 (1)
12 (5)	7 (5)	4 (4)	4 (4)	-4 (2)	-3 (2)
24 (18)	57 (23)	2 (2)	32 (13)	-3 (7)	-4 (7)
12 (3)	12 (3)	10 (4)	-3 (4)	-4 (3)	3 (5)
17 (6)	13 (6)	11 (5)	0 (5)	1 (3)	2 (3)
11 (5)	7 (5)	15 (5)	2 (3)	1 (3)	7 (4)
11 (17)	43 (21)	2 (1)	6 (9)	-6 (6)	-9 (7)
22 (5)	13 (5)	0 (4)	0 (3)	-3 (3)	5 (4)
14 (3)	13 (3)	2 (3)	7 (4)	1 (2)	-5 (3)
21 (3)	12 (3)	10 (4)	1 (5)	-5 (2)	1 (4)
28 (9)	28	9 (3)	14	0	0
15 (3)	8 (2)	9 (3)	4 (3)	-3 (2)	-2 (3)
23 (8)	23	6 (2)	11	0	0
7 (3)	13 (3)	7 (2)	-2 (2)	-2 (2)	-2 (2)
18 (8)	24 (9)	4 (1)	9 (7)	-2 (3)	-2 (3)
15 (3)	18 (3)	4 (3)	-3 (2)	3 (2)	2 (2)
24 (9)	35 (10)	3 (1)	14 (8)	-1 (3)	-3 (3)
13 (3)	14 (3)	8 (3)	2 (2)	0 (2)	2 (2)
25 (9)	30 (9)	1 (1)	-5 (8)	-1 (3)	-1 (2)
13 (3)	11 (3)	9 (3)	-1 (2)	-1 (2)	-3 (2)
49 (11)	12 (8)	3 (1)	11 (8)	1 (3)	3 (2)
8 (3)	13 (3)	12 (3)	-4 (2)	0 (2)	1 (2)
17 (3)	15 (3)	10 (3)	5 (2)	-2 (2)	-2 (2)
18 (3)	14 (3)	4 (3)	-5 (2)	3 (2)	-3 (2)
19 (3)	6 (3)	14 (3)	3 (2)	0 (2)	2 (2)
17 (3)	8 (3)	2 (3)	-1 (2)	1 (2)	-3 (2)
16 (3)	10 (3)	4 (3)	4 (2)	0 (2)	1 (2)
16 (3)	11 (3)	5 (3)	-1 (2)	-1 (2)	0 (2)
17 (3)	10 (3)	9 (3)	0 (2)	-4 (2)	-1 (2)

* Error in parentheses is one standard deviation; for 0.0241 (1) read 0.0241 ± 0.0001 , etc. β_{ij} are given times 10^4 . Temperature factor form $\exp \left\{ - \sum_{i=1}^3 \sum_{j=1}^3 h_i h_j \beta_{ij} \right\}$.

compared with the observed in Table 3. The thermal ellipsoid data are presented in Table 4 for boracite only.

Table 3. Comparison of observed and calculated structure factors.
A. Boracite. * indicates "less-than" reflections

h	k	l	F _o	F _c	h	k	l	F _o	F _c	h	k	l	F _o	F _c	h	k	l	F _o	F _c	h	k	l	F _o	F _c
1	0	0	0.3*	0.0	13	6	0	0.9*	4.4	3	14	0	7.8	7.5	5	7	1	26.7	26.1	13	0	1	2.2*	0.0
2			18.2	14.2	14			14.5	14.7	4			23.2	22.2	7			44.9	44.5	12			8.6	8.9
3			0.4*	0.0	14	7	0	0.9*	3.5	5			0.9*	0.6	8			5.2*	5.1	11			0.8*	0.0
4			117.8	130.8	13			27.2	26.2	5			24.8	24.6	11			15.2	14.9	10			48.7	48.1
5			0.7*	0.0	12			0.9*	2.2	7			1.0*	2.4	10			19.3	18.7	9			1.5*	0.0
6			6.1	4.0	11			0.8*	0.9	8			19.5	19.3	11			10.5	10.5	8			5.6	7.7
7			2.7*	0.0	10			8.1	6.2	9			5.2*	4.3	12			7.3	5.4	7			0.6*	0.0
8			55.5	55.9	9			26.5	27.8	9	14	1	13.1	12.9	13			9.2	8.9	6			54.8	54.6
9			2.3*	0.6	8			0.7*	0.9	8			1.0*	0.0	14			9.9	9.7	5			0.5*	0.0
10			25.5	26.2	7			74.0	75.3	7			8.0	9.2	14	6	1	0.9*	5.1	4			10.8	10.4
11			0.8*	0.0	6			0.7*	1.2	6			16.2	16.9	13			8.3	9.4	3			0.4*	0.0
12			39.5	38.7	5			22.7	23.7	5			10.5	10.2	12			25.4	25.1	2			37.0	37.0
13			0.9*	0.0	4			8.5	8.4	4			0.9*	0.7	11			21.8	21.5	1			0.3*	0.0
14	1	0	0.9*	0.1	3			33.2	33.2	2			14.2	15.7	10			11.4	12.2	9			0.3*	0.0
15			4.6*	6.1	2			0.6*	0.6	1			0.9*	1.4	9			13.3	13.1	0	0	2	48.1	54.1
16			0.3*	2.5	1			0.6*	1.8	0			0.9*	0.0	8			12.2	13.6	1			0.4*	0.0
17			7.5	9.1	0			13.9	11.9	0	13	1	0.9*	0.0	7			1.7*	0.8	3			0.4*	0.0
18			1.0	1.0	0	8	0	73.5	74.2	1			7.0*	8.9	6			22.4	21.3	4			2.0*	3.6
19			17.2	16.8	1			10.1	10.1	2			0.9*	5.3	5			0.6*	1.4	5			0.5*	0.0
20			2.2*	3.4	2			64.1	64.9	3			11.4	12.2	4			33.2	32.9	6			49.7	49.0
21			0.6*	1.7	3			4.5*	3.7	4			6.7*	9.0	3			39.2	38.6	7			0.6*	0.0
22			13.8	13.7	4			66.5	66.0	5			17.4	17.0	2			0.6*	4.6	8			21.1	21.0
23			58.1	58.9	5			0.7*	2.3	6			10.3	11.0	1			39.3	39.3	9			0.7*	0.0
24			7.4	6.1	6			4.7*	7.3	7			5.1*	8.8	0			0.7*	8.8	7			35.3	35.7
25			74.3	75.6	7			0.7*	1.1	8			13.1	13.9	0	5	1	0.5*	0.0	11			0.7*	0.0
26			1.9*	0.6	8			25.1	24.1	9			10.9	13.0	1			48.7	48.7	12			49.4	48.6
27			47.0	50.6	9			0.8*	1.1	10			1.0*	2.3	2			46.4	44.2	13			0.9*	0.0
28			0.0	0.5	10			5.9*	6.2	11	12	1	1.0*	0.4	3			29.8	29.0	14			19.1	18.7
29	0	2	0	0	11			9.2	8.8	10			8.3	9.9	4			4.0*	0.0	14	1	2	1.5*	0.0
30			3.4*	2.4	12			31.9	31.4	9			15.0	12.9	5			36.1	35.7	13			17.1	17.9
31			3.4*	1.7	13			12.7	13.3	8			19.4	20.1	6			0.6*	2.3	12			0.8*	0.8
32			29.6	27.9	14			0.9*	5.5	7			8.7	8.0	7			17.8	17.5	11			12.9	14.1
33			5.2	5.2	14			1.0*	5.6	6			7.6	8.3	8			15.7	14.8	10			6.9	7.5
34			108.4	111.2	13	9	0	3.2*	5.5	5			11.1	10.6	9			40.3	38.7	9			22.2	22.9
35			2.3*	3.4	12			0.9*	3.9	4			7.7	10.4	10			5.8	3.6	8			3.0*	3.8
36			15.4	13.4	11			0.9*	3.1	3			11.1	12.3	11			1.0*	4.5	7			20.4	19.0
37			5.7	5.9	10			5.0*	3.8	2			0.8*	2.2	12			0.8*	4.9	6			4.0*	6.0
38			45.9	44.3	9			41.8	39.9	1			6.7	5.6	13			14.6	12.7	5			30.8	28.8
39			4.2*	6.4	8			0.8*	0.5	0			0.8*	0.0	14			3.4*	3.8	4			6.2	5.9
40			32.5	32.1	7			9.2	8.3	0	11	1	5.5*	0.0	14	4	1	14.5	15.7	3			54.7	50.8
41			0.8*	2.2	6			0.8*	2.4	1			14.6	15.6	13			16.3	12.2	2			0.4*	1.7
42			9.6	10.9	5			35.9	35.4	2			4.3*	7.4	12			14.6	14.9	1			16.7	14.1
43			0.9*	7.8	4			1.0*	5.6	3			31.4	3.1	11			20.1	17.6	0			0.3*	0.8
44	3	0	0.8*	1.0	3			21.4	20.9	4			19.8	20.1	10			29.1	29.0	2	2	2	72.9	74.2
45			4.6*	3.7	2			0.7*	0.2	5			11.8	12.2	9			15.1	16.0	1			0.4*	0.7
46			21.2	20.3	1			38.8	38.6	6			22.0	22.3	8			9.7	10.2	2			86.4	88.3
47			6.9	7.0	0			0.8*	5.6	7			22.5	22.1	7			13.3	13.6	3			10.9	10.1
48			0.7*	0.6	10	0		56.5	56.6	8			20.5	19.9	6			45.7	44.4	4			91.3	91.3
49			5.5	4.7	1			2.0*	1.8	9			9.1	11.4	5			5.3	5.3	5			5.7	5.7
50			32.8	32.1	2			33.8	33.8	10			0.9*	3.8	4			5.2	5.0	6			9.9	8.7
51			11.0	11.2	3			7.5	8.5	11			1.0*	7.6	3			0.5*	2.7	7			11.2	11.3
52			58.2	55.9	4			12.9	12.4	12			0.9*	1.4	2			21.6	21.7	8			21.7	20.9
53			0.4*	1.7	5			3.9*	1.2	13	10	1	0.9*	1.2	1			105.5	104.1	9			5.9	8.3
54			29.8	33.0	6			37.2	36.8	12			6.4*	9.5	0			0.5*	0.0	10			9.7	9.7
55			0.4*	0.6	7			0.8*	4.0	11			0.9*	3.1	0	3	1	0.4*	0.0	11			5.6*	4.4
56			92.2	94.6	8			0.8*	5.5	10			19.8	19.2	1			30.3	30.5	12			10.0	12.0
57			2.8*	4.2	9			3.7	3.7	9			0.9*	5.6	2			7.2	6.9	13			0.8*	0.7
58	4	0	117.0	123.0	10			1.0*	5.8	8			8.1	8.8	3			55.5	54.8	14			8.1	10.8
59			4.5	4.2	11			0.9*	1.5	7			11.9	12.0	4			2.8*	2.7	14	3	2	42.7	42.0
60			35.2	33.4	12			0.9*	3.6	6			21.2	19.8	5			7.0	7.5	13			27.4	25.2
61			0.5*	4.4	13			0.9*	1.7	5			0.8*	2.0	6			43.3	42.2	12			0.8*	1.3
62			95.2	96.9	12	0		3.5*	0.6	4			2.9*	6.9	7			31.5	30.1	11			12.0	12.1
63			0.6*	1.2	11			1.0*	5.1	3			22.5	21.5	8			33.3	33.9	10			7.4	8.8
64			21.3	20.9	10			0.9*	2.1	2			4.2*	7.1	9			23.7	23.0	9			31.2	31.3
65			3.7*	4.8	9			0.9*	0.6	1			17.2	16.8	10			18.0	17.6	8			0.7*	4.4
66			59.2	59.2	8			3.6*	3.0	0			0.7*	0.0	11			14.1	15.7	7			36.2	37.4
67			3.4*	4.2	7			11.5	11.3	0	9	1	1.9*	0.1	12			6.9	7.4	6			12.5	12.2
68			18.2	17.9	6			36.0*	35.2	1			35.9	31.6	13			12.6	13.6	5			41.8	41.4
69			10.9	12.1	5			21.9	21.6	2			27.9	28.4	14			8.2	8.6	4			4.6*	4.2
70			35.0	33.7	4			0.8*	1.4	3			18.8	19.6	14	2	1	1.8*	6.6	3			34.2	31.8
71			5.2*	9.0	3			35.7	34.9	4			10.4	10.5	13			9.4	8.2	2			9.6	9.4
72			19.0	18.0	2			0.8*	3.1	5			38.8	39.1	12			30.7	29.6	1			72.0	70.2
73	5	0	5.3*	6.3	1			8.1	6.6	6			16.0	15.1	11			4.9*	8.6	0	4	2	29.8	28.3
74			7.4	8.7	0			0.9*	1.8	7														

Table 3A. (Continued)

h	k	l	F _o	F _c	h	k	l	F _o	F _c	h	k	l	F _o	F _c	h	k	l	F _o	F _c	h	k	l	F _o	F _c
2	5	2	0.5*	2.8	10	12	2	4.2*	5.1	12	8	3	11.7	9.9	2	2	3	12.7	12.7	10	4	4	11.6	12.6
1			47.7	45.5	11			0.9*	2.2	11			0.9*	4.2	1			3.5*	3.3	11			4.5*	5.0
0			12.5	12.1	10	13	2	1.0*	3.8	10			15.7	14.6	0			0.4*	0.0	12			35.6	32.2
0	6	2	16.3	16.2	9			8.6	6.6	9			15.2	16.7	0	1	3	0.4*	0.0	13			0.9*	3.5
1			4.9	4.0	8			0.9*	2.0	8			19.5	18.6	1			23.6	24.0	14			15.0	12.7
2			37.2	38.1	7			9.2	9.6	7			15.5	15.5	2			3.6*	2.8	14	5	4	3.2*	3.0
3			2.9*	6.0	6			0.9*	8.1	6			10.7	11.1	3			4.7	4.0	15			17.6	19.4
4			6.7	5.1	5			13.9	12.8	5			0.7*	1.1	4			2.2*	4.1	12			0.9*	1.9
5			3.5*	4.2	4			5.6*	4.5	4			21.0	21.7	5			52.2	51.3	11			0.8*	4.0
6			25.9	26.3	3			25.9	26.3	3			33.5	33.4	6			25.3	24.6	10			8.4	9.9
7			0.7*	1.5	2			4.8*	5.5	2			5.9	6.3	7			30.6	30.8	9			25.4	24.5
8			36.5	36.9	1			17.7	18.5	1			31.7	32.3	8			32.7	32.6	8			3.5*	1.2
9			0.8*	3.2	0			6.0*	5.1	0			3.9*	0.0	9			31.1	31.6	7			4.6*	5.2
10			0.8*	3.1	0	14	2	7.2*	8.8	0	7	3	0.6*	0.0	10			18.6	17.2	6			10.1	10.8
11			0.8*	2.4	1			0.9*	2.7	1			39.0	38.9	11			28.3	28.5	5			34.3	32.4
12			11.5	9.8	2			18.2	18.8	2			16.9	18.9	12			7.0	8.5	4			0.6*	1.9
13			3.0*	1.3	3			0.9*	2.0	3			45.1	45.8	13			10.9	11.6	3			17.9	18.6
14			8.0	7.1	4			15.7	16.9	4			0.6*	4.9	14			15.9	15.1	2			8.4	7.8
14	7	2	0.9*	3.2	5			0.9*	5.7	5			12.7	12.4	14	0	3	25.3	25.1	1			57.9	57.5
13			19.3	19.5	6			16.3	15.2	6			13.7	13.8	13			0.8*	0.0	0			4.5	3.3
12			0.9*	5.8	7			3.5*	1.8	7			37.9	37.0	12			10.9	12.4	0	6	4	33.7	32.7
11			7.5	8.4	8			16.2	16.2	8			11.2	12.0	11			0.8*	0.0	1			5.4*	0.5
10			0.8*	2.7	9			1.0*	0.4	9			8.7	8.6	10			35.9	35.5	2			120.4	125.6
9			10.4	10.6	9	14	3	1.0*	7.1	10			0.8*	2.9	9			0.7*	0.0	3			0.6*	1.1
8			2.9*	5.4	8			5.5*	1.6	11			33.1	32.4	8			13.6	13.4	4			40.5	40.0
7			3.6*	4.7	7			7.5	7.9	12			0.9*	5.6	7			0.6*	0.0	5			6.9	6.6
6			0.7*	3.3	6			12.0	12.4	13			10.3	12.4	6			39.3	39.6	0			64.3	65.0
5			39.2	39.5	5			9.4	10.6	14	6	3	7.2*	7.8	5			0.5*	0.0	7			0.6*	0.7
4			6.3	7.2	4			0.9*	6.8	14	6	3	11.5	11.3	4			19.2	18.3	8			21.7	21.4
3			28.8	27.8	3			13.4	12.2	13			4.0*	5.5	3			0.5*	0.0	9			5.0*	4.0
2			2.2*	3.6	2			0.9*	4.3	12			16.4	15.7	2			44.1	44.0	10			15.2	12.8
1			35.9	35.8	1			11.7	12.1	11			9.9	10.2	1			2.4*	3.0	11			0.8*	2.2
0	8	2	7.8	7.4	0			0.9*	0.0	9			0.8*	2.1	0	4		0.4*	0.0	12			15.8	15.9
1			6.8	6.6	1			19.2	18.1	8			40.0	39.7	2			0.4*	0.0	13			10.4	9.7
2			23.7	25.3	2			6.3*	8.6	7			11.0	12.2	3			0.4*	0.0	14	7	4	4.9*	3.1
3			0.7*	4.2	3			7.0*	4.0	6			9.9	10.2	1			0.5*	0.0	15			23.9	22.6
4			8.8	7.7	4			8.5	10.4	5			14.5	15.2	6			63.0	61.7	12			4.6*	1.0
5			0.7*	1.7	5			21.6	20.1	4			19.4	19.2	7			4.1*	0.0	11			13.2	14.9
6			17.1	16.8	6			5.7*	5.8	3			0.6*	1.4	8			79.7	79.8	10			0.8*	3.8
7			7.2	7.9	7			7.5	8.2	2			14.0	14.0	9			0.7*	0.0	9			0.8*	5.8
8			22.7	22.0	8			0.9*	2.3	1			23.2	22.3	10			3.6*	4.4	8			0.8*	3.7
9			7.2	6.9	9			15.8	17.2	0			0.6*	0.0	11			0.8*	0.0	7			32.3	31.9
10			11.4	13.1	10			1.0*	1.4	0	5	3	0.5*	0.0	12			32.7	31.2	6			0.7*	6.4
11			5.4*	8.2	11	12	3	1.0*	2.3	1			49.7	50.2	13			0.8*	0.0	5			20.5	19.4
12			6.2*	9.7	10			0.9*	2.5	2			3.7*	4.4	14			7.8	7.2	4			4.6*	3.6
13			3.0*	4.4	9			0.9*	4.1	3			31.6	30.9	14	1	4	0.9*	3.6	3			65.5	65.6
14			1.0*	5.4	8			27.3	26.6	4			45.8	45.3	13			12.0	12.5	2			8.2	8.1
14	9	2	0.9*	7.7	7			9.0	8.9	5			57.0	56.5	12			0.8*	2.5	1			23.4	22.2
13			12.2	12.4	6			0.9*	1.4	6			13.3	13.1	11			11.0	12.0	0			9.7	10.5
12			0.9*	3.3	5			0.9*	4.1	7			14.3	14.3	10			3.2*	4.4	0	8	4	76.3	77.2
11			34.5	33.6	4			13.0	14.2	8			1.6*	2.1	9			30.2	29.6	1			0.7*	2.0
10			0.9*	7.1	3			10.8	11.0	9			30.9	30.0	8			4.8*	7.1	2			39.6	40.2
9			0.8*	5.5	2			8.4	8.4	10			24.9	24.0	7			24.6	23.8	3			9.5	9.6
8			0.8*	2.4	1			7.7	8.9	11			27.3	26.8	6			2.6*	3.5	4			54.3	52.8
7			19.0	18.8	0			0.8*	0.0	12			2.0*	3.5	5			63.5	62.2	0			5.0*	2.4
6			7.5	7.8	0	11	3	0.8*	0.0	13			18.8	19.4	4			0.5*	0.5	6			20.6	20.8
5			25.3	24.5	1			25.4	24.7	13			12.0	13.6	3			23.9	21.2	7			6.5	7.6
4			0.7*	4.3	2			21.3	21.0	14	4	3	25.6	25.9	2			3.6*	3.4	8			36.6	35.5
3			22.9	23.5	3			23.2	23.2	15			12.3	12.9	1			82.8	84.3	9			4.5*	6.8
2			0.7*	3.5	4			18.7	18.7	12			0.8*	1.4	0			2.1*	3.1	10			12.3*	1.5
1			7.9	9.6	5			10.0	10.0	11			19.5	21.2	0	2	4	46.8	44.8	11			0.9*	2.1
0			9.2	8.2	6			13.0	12.5	10			36.7	36.4	1			4.7	4.5	12			25.9	25.2
0	10	2	23.3	22.6	7			22.8	22.7	9			20.3	20.7	2			118.2	127.5	13			0.9*	2.7
1			4.5*	2.2	8			0.9*	4.9	8			16.4	16.6	3			1.5*	4.4	14			12.6	8.5
2			7.4	6.0	9			13.4	13.5	7			3.7*	4.3	4			29.6	27.9	13	9	4	24.8	23.8
3			8.1	8.8	10			10.3	11.2	6			33.4	33.3	5			0.5*	3.3	12			1.8*	5.9
4			19.7	19.7	11			24.2	24.9	5			38.8	37.6	6			123.3	128.3	11			16.9	16.5
5			0.8*	4.8	12			4.1*	5.1	4			16.4	15.3	7			7.0	6.9	10			0.9*	6.2
6			14.1	15.5	13	10	3	0.9*	1.6	3			43.0	40.9	8			22.4	21.2	9			0.9*	6.5
7			6.8	8.3	12	5		0.9*	2.0	2			13.8	13.5	9			6.6	4.7	8			5.2*	3.7
8			12.9	13.7	11			9.9	7.2	1			5.5	5.0	10			35.4	34.5	7			9.0	8.2
9			9.9	11.3	10			21.3	20.5	0			0.5*	0.0	11			4.0*	6.4	6			7.4	8.5
10			8.6	7.1	9			26.6	26.9	0	3	3	0.5*	0.0	12			17.3	17.0	5			14.6	14.6
11			4.7*	3.9	8			20.1	19.4	1			19.4	19.8	13			6.						

